

Simple Fault Path Indication Techniques for Earth Faults

Matti Lehtonen, Osmo Siirto, and Mohamed F. Abdel-Fattah

Abstract—Fault indication is the key element in any fault management system. In case of short circuits, fault indication is straightforward, but especially in ungrounded and compensated neutral networks, the single phase fault currents are typically so small that simple fault current threshold detection hardly gives any satisfactory results. The problem can be solved by combining neutral voltage measurement to the sum current measurement using directional relay characteristics. However, the requirement of both current and voltage measurements makes the solution cost prohibitive especially when retrofitting in the existing secondary substations. Hence, there is the need for a simple but reliable earth fault indicator which is based on current measurements solely. This paper takes the above mentioned challenge and compares a number of possible fault indication solutions which are using local current measurements at the secondary substations only. The methods presented use either the sum current measurement directly, or are based on the comparison of the measured phase currents using symmetrical components.

Index Terms—Earth fault, fault indication, unearthed and compensated neutral and medium voltage cable networks.

I. INTRODUCTION

Indication of the fault current passage is the key element in any fault management system, including the self-healing functions of smart grids. In case of multi-phase faults, the fault levels are typically high, and the fault indication can be simply based on phase current measurement and threshold detection. Unfortunately this is not the case with earth faults. Especially in ungrounded and compensated neutral networks, the single phase fault currents are typically so small, and the dynamics of the fault current range required so high, that simple fault current level detection hardly gives any satisfactory results.

In protective relaying, this problem has been solved by combining neutral voltage measurement to the sum current measurement using directional relay characteristics. In ungrounded networks, the direction of capacitive current is used, and it gives a very good performance since in faulty and sound line sections the capacitive currents are in 180° phase shift compared to each other. In compensated neutral systems, the capacitive currents may have any direction and the above principle cannot be used as such. Instead, the directional measurement uses the resistive component of the

fault current. Since this component is very small, it is usually artificially increased by temporarily connecting a resistor parallel to the compensation coil.

A very good fault passage indicator can be implemented using the same principles as the protective relays use. However, the requirement of both current and voltage measurements makes the solution cost prohibitive in many cases, especially when retrofitting. The current measurements are relatively easy to arrange using e.g. Rogowski coils, but the critical factor is the voltage measurement, which is in many cases expensive and tedious to install in the already existing secondary substations. Hence, there is the need for a simple but reliable earth fault indicator which is based on current measurements solely.

This paper takes the above mentioned challenge and compares a number of possible fault indication solutions which are using local current measurements at the secondary substations only. The methods presented use either the sum current measurement directly, or are based on the comparison of the measured phase currents using symmetrical components. In the following, in section II, the fault indication methods considered are first presented. In section III, their role in automation and fault management is discussed from the city or urban medium voltage distribution network point of view. In section IV, the fault indication methods are tested by simulated data, and section V discusses the use and implementation of the methods. Section VI finally makes a conclusion of the paper.

II. EARTH FAULT INDICATION METHODS

This section presents the suggested earth fault indication methods. What is common to the methods is that they only use local current measurements at the secondary substations, and they are planned to be used in medium voltage distribution networks with either ungrounded or compensated neutral. First of the methods utilizes the peak of the initial transient of the earth fault current. The second utilizes the stepwise change of the sum current when the additional resistance is connected in parallel to the compensation coil, whereas the third method is based on the comparison of the changes in symmetrical components of the currents.

A. Method 1

In the beginning of the ground fault there are three transients, initiated by discharging the faulty phase, charging the two healthy phases and by energizing the compensation coil. The discharge and charge transients have the frequency of 500–2500 Hz and 100–800 Hz, respectively and they are similar in ungrounded and compensated neutral systems. Of these two, the charge component is the dominating one having lower frequency and higher amplitude. In

M. Lehtonen is with the Department of Electrical Engineering, Aalto University, FI-02150 Espoo, Finland (e-mail: matti.lehtonen@aalto.fi).

M. F. Abdel-Fattah is with the Department of Electrical Engineering, Aalto University, FI-02150 Espoo, Finland and with the Department of Electrical Power and Machines Engineering, Zagazig University, Sharqia, PO Box 44519, Egypt (e-mail: mohamed.f.abdelfattah@gmail.com).

O. Siirto is with the Helen Electricity Network Ltd., Helsinki, Finland (e-mail: osmo.siirto@helen.fi).

compensated neutral systems, there is in addition the coil energizing transient, which at low fault resistances comprises a decaying DC component and but appears as a rising amplitude fundamental frequency when the fault resistance is increased.

An example of the phase currents during an earth fault in a medium voltage distribution system is given in Fig. 1. The fault has low resistance and the network is fully compensated using a Petersen coil. The transient current is clearly seen in the faulty phase, whereas the other two phases only have a small transient component, which hardly is observable. The transient currents in the two healthy phases are composed of the fraction of the total earth fault current which closes the circuit through the phase capacitances of these two phases in the faulty feeder. Since the network has full compensation, the continuous fault current is very small and can hardly be detected after the transient has attenuated. To the contrary, the transient amplitude is typically very high compared to the fundamental frequency fault current, and is typically 10–20 times higher than the uncompensated capacitive fault current. This feature makes the transient very attractive for earth fault indication purposes.

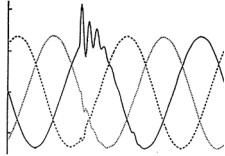


Fig. 1. An example of the earth fault initial transient currents in a medium voltage network (vertical axis – time, horizontal axis – phase currents).

The first method utilizes the peak of the initial transient of the earth fault current for fault indication. The transient peak amplitude depends on the location of the measurement as follows:

$$i = i_F \frac{C_{tot} - C_l}{C_{tot}} \quad (1)$$

Where i_F is the fault current in the fault location, measured as sum or zero component current, i is the sum or zero sequence current measured in line locations before the fault, C_{tot} is the total earth capacitance of the network and C_l is the earth capacitance of the line sections behind the measurement point. Hence, for instance, if we are moving the measurement point along the line, the current amplitude is increased towards the fault location, due to a smaller share of earth capacitances being behind the measurement point.

In a similar way, if the measurement point is behind the fault, the measured sum current comprises only the fraction of total fault current that is closed through the capacitances behind the measurement point:

$$i = i_F \frac{C_l}{C_{tot}} \quad (2)$$

Usually C_l is much smaller than C_{tot} , which makes the differentiation between the two cases in (1) and (2) easier. However, the setting of threshold level of fault indication between these two cases is not straightforward due to large dynamics of the fault current amplitude. If the fault is initiated at phase voltage instantaneous zero, the transient is only a small fraction (5%–10%) of the maximum case. Also,

if there is a substantial degree of fault resistance, the fault current is further decreased. As a consequence, there hardly is any fixed value where the setting could be made so that the fault indication could be selective in all the practical situations.

The solution to the above problem is to make the fault indication setting dynamic. This leads to the following procedure:

Step 1: Fault is detected by the primary substation relays and the faulty line is detected, or in most practical cases disconnected by the circuit breaker operation.

Step 2: The fault management system collects the measured currents from all the fault indicators accessible in the affected line.

Step 3: The current measurement with the highest amplitude is found, and all the measurements are scaled by this amplitude. Now we have the fault indications as per unit values, the highest indication being the one closest to the fault.

Step 4: The fault indicator outputs are next obtained by the following rules: If the measured p.u. current is higher than $(1-m)$, where m is the per unit margin, the fault is behind the measurement concerned and the fault indication is “TRUE”, and correspondingly, if the measured current is under this threshold value, the fault indication is “FALSE”.

Step 5: The fault indications are compared with each other to see whether there is common agreement of the fault location. For reliable fault location, there should not be contradicting fault indications.

The next question is, how the margin in the *Step 4* should be selected. The approach proposed here is to use the average value in the middle of theoretically correct indications in the beginning of the faulty feeder, i.e.

$$m = \frac{C_{tot} - C_l}{2C_{tot}} \quad (3)$$

This setting divides the impact of measurement errors equally between the “TRUE” and “FALSE” cases, and is assumed to give a practically sound result. The sensitivity of this setting is discussed more in the section IV.

B. Method 2

In compensated neutral systems, the fault current is typically so small that, for reliable relay operation, it must be artificially increased by a temporary connection of an additional neutral resistance parallel to the compensation coil. The resistance is usually connected after a delay, in order to allow some time for fault arc self-extinction. The second method utilizes the stepwise change of the sum current when the additional resistance is connected. The rating of the resistor is typically such, that with a full earth fault (100% neutral voltage), the resistive current produced is 5 A or 10 A.

The behavior of fault current in a compensated network with additional resistor switching is depicted in Fig. 2. In the beginning of the fault, a transient can be observed, which in this particular case mostly comprises the coil circuit initial transient. After initial transients the currents settle down at approximately 0.5 second, and the resistor is switched on at the 1.0 second time.

The Method 2 is based on the difference of the fault current before and after the resistor switching moment. The solution procedure is similar to the Method 1, with the

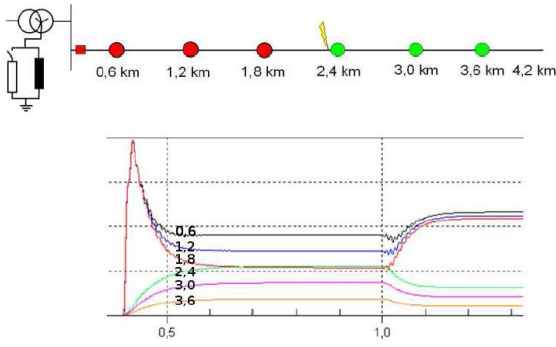


Fig. 2. The earth fault currents in a compensated network (vertical axis – time, horizontal axis – fault current 10 ms average values) [13].

difference that for making comparisons of the measurements, the phasor change of the fault currents are used:

$$\Delta I_{sum} = I_{sum}(t + n\tau) - I_{sum}(t) \quad (4)$$

where t is the time a few cycles before resistor switching, τ is the time of one power system cycle (20 ms) and $n\tau$ provides a synchronous time difference, when n is an integer. Note that current I must be expressed as a phasor, having both amplitude and phase angle. The time before switching and the number of cycles n should be selected such that the fault current is stable after the changes or initial transients. Now the fault indication procedure is as follows:

Step 1: Fault is detected by the primary substation relays and the faulty line is detected.

Step 2: The fault management system collects the measured currents from all the fault indicators.

Step 3: The parameters t and n are defined for all the measurements and current changes are calculated according to (4). Current measurement with the highest change in amplitude is found, and all the measurements are scaled by this amplitude. Now we have the fault indications as per unit values, the highest indication being the one closest to the fault.

Step 4: The fault indicator outputs are next obtained by the similar rules as in case of Method 1. However, the setting of the margin can't be defined in that straightforward way, since the current changes in the network earth capacitances depend on the sharpness of the compensation circuit resonance and on how earth capacitances are divided round the network. However, the current fractions changes in the earth capacitances are relatively small, and we may use a rough estimate $m = 0.5$ for the margin.

C. Method 3

The third fault indication method utilizes the changes in symmetrical component currents during the fault initiation. Basically, the earth fault existence can be detected by observing an increase in zero sequence current. However, with regard to the selective fault path indication, the change of the zero sequence current alone is not enough, due to the earth fault currents returning through the earth capacitances behind the fault location. This problem can be solved by measuring also the change in negative sequence component current and comparing it to the simultaneous change in zero sequence current.

In the fault point, all the three symmetrical components of fault current are equal. Along the fault current path between the feeding substation and the fault point, the negative

sequence component varies only a little, but it is practically non-existent behind the fault. To the contrary, the zero sequence component has a similar behavior as is described by (1) and (2). This difference in behavior can be utilized for the selectivity of the fault indication as follows:

Step 1: The existence of an earth fault is detected, if the change in zero sequence current is higher than the set threshold value:

$$\Delta I_0 > \Delta I_{0,set} \quad (5)$$

Step 2: The change in negative sequence current is computed. The measurement point is along the fault current path, if the following condition is satisfied:

$$\Delta I_n > \Delta I_0(1-m) \quad (6)$$

Hence, if both the conditions, (5) and (6) are satisfied, the fault indication is "TRUE", otherwise it is "FALSE".

The performance of the method is defined by two parameters, the set current threshold value and the margin. For high impedance faults, the fault current amplitude is governed by the fault resistance and can be approximated simply by Ohms' law, i.e. for 10 k Ω fault resistance and 20 kV network, the fault current would be about 1.2 A and the zero sequence current respectively round 0.4 A. Now we still need to define the margin m in (6). At the fault point, the two component currents are equal, but towards the feeding primary substation, the zero component is decreased whereas the negative sequence component has a slight variation only. As a consequence, the negative sequence component gradually grows higher than the zero sequence component, and it is quite safe to take a small margin. In this paper, a value $m = 0.2$ was taken.

Method 3 is simpler compared to the other two methods in the sense, that it does not require comparison of measurements in different network locations. Hence it would be a preferred choice for fault indication in the cases where decentralized fault management is implemented.

When assessing the accuracy of the considered methods, some assumptions were made. In the case of Method 1, the result was considered reliable, if the following condition was satisfied:

$$I_r \varepsilon < I_{meas} m \quad (7)$$

where I_r is the rated current of the current transformer (taken 100 A), ε is the p.u. current amplitude error (taken as 0.01), I_{meas} is the measured peak amplitude of the transient current, and the margin is $m = 0.4$ as obtained by summing the capacitances of the feeder A versus the total network. For the other two methods, the (7) was used with the margins $m = 0.5$ and $m = 0.2$ for the Methods 2 and 3, respectively. To finalize the parameters, the threshold value of zero sequence current change in Method 3, (5) was set to 0.4 A.

III. USE OF THE FAULT LOCATION METHODS

This section discusses the practical use and application of the developed techniques. The role of the simple fault indication as a part of comprehensive fault management in urban and city environments is clarified. As an example case, the medium voltage distribution network of Helsinki is used.

Helen Electricity Network Ltd. (Helen) is the distribution network operator in Helsinki. Helsinki is the capital of Finland with a lot of government offices and business headquarters. Service and commercial customer groups are using over half of the electricity. The customer interruption cost (CIC) studies both in Finland and internationally indicate significant outage damage in those customer groups [1]–[4]. Hence, high reliability of the supply in Helsinki is appreciated. Distribution automation (DA) has been chosen as an effective mean to improve the reliability and reduce CIC.

DA in Helsinki includes remote controls, alarms, state monitoring and fault indications, as well as power quality, power component temperature and load measurements. There are over 2400 secondary substations and an optimization study [5] revealed 14 to 33 % coverage of fully automated secondary substations, depending on the CIC values in the corresponding feeder. A typical distribution automation layout structure used in Helsinki city core is described in Fig. 3. In city areas, the network is of underground cable construction with unearthed neutral.

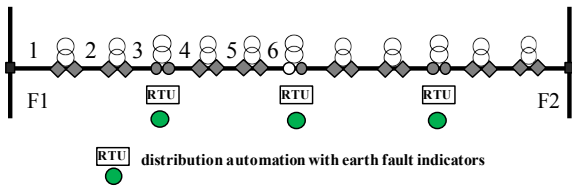


Fig. 3. A typical distribution automation layout, automation in normally open point and on half-way sections of the feeders.

Consider an earth fault on Feeder 1 (F1) of Fig. 3. The best benefit from distribution automation can be achieved if the control centre receives the information about exact and reliable location of the fault either from distribution automation system or from other sources. If the exact location is not known, the rapid utilization of the distribution automation depends on whether the earth fault is before or after the automated secondary substation. If the earth fault is before the first automation point, the supply can be restored to the customers between sections 4 to 6 using remote controllable switches. If the fault is behind the first automation point, the fast restoration of the supply is not utilized, because trial and error controls are needed to find the exact location of the fault. These would produce new interruptions on recently restored customers and consecutive power on-off situations. The location of the earth fault is search by moving the open point from normally open point to another location on feeder 1. The protection will trip the feeder, if the fault is before the new location. When the right section (1, 2 or 3) is found, the fault is isolated the supply is restored to all of the customers.

The need to use trial and error switching actions to locate the earth faults substantially decreases the benefits of distribution automation. If distribution automation would cover all the secondary substations, the exact location of the fault would be known and trial switching would be avoided. Since 100% coverage of distribution automation is a very expensive solution, there is a need for a more affordable solution to locate the faulty sections accurately. One solution is to complement the fully automated substations with a comprehensive fault indication solution. In this solution, in every secondary substation between the fully automated substations, there are fault passage indicators (FPI), both

short-circuit indicators and earth-fault indicators. Besides fault passage indicators, a low-cost communication device is needed to pass this information to the control center. With this solution, the fast fault location, isolation and restoration process would be possible in all medium voltage feeder faults. An example of the placing of the fault passage indicators and distribution automation is described in Fig. 4.

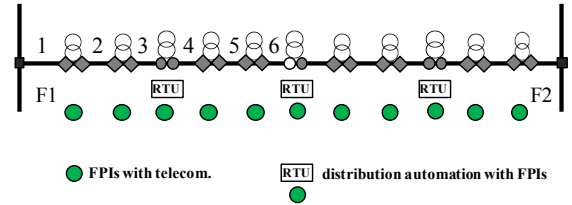


Fig. 4. The placing of fault passage indicators (FPI) with telecommunication and distribution automation.

The illustrated comprehensive fault location and distribution automation layout enables rapid utilization of DA on all faults regardless of the section where an earth fault emerges. The proposed method will eliminate the need of harmful and stressful trial and error switching actions and will accelerate the fault management process.

IV. TESTING OF THE ALGORITHMS

The three suggested algorithms were tested using a test network and simulated data. Based on the experience of the current situation of the 20 kV medium voltage cable distribution networks, a realistic network arrangement is proposed for the study. The simulated network is presented in Fig. 5.

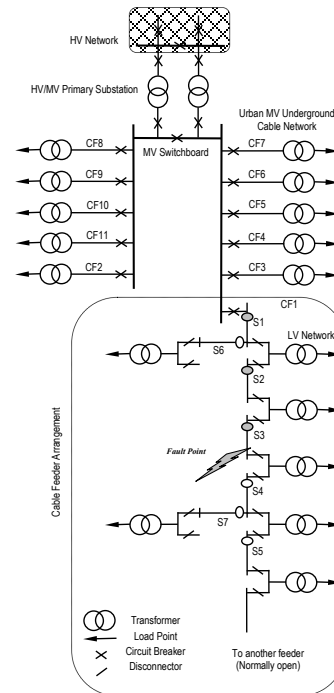


Fig. 5. The simulated network.

Based on Fig. 5, the faulted feeder (CF1) consists of five looped sections (S1–S5) and other two extra branched sections (S6 and S7) have been added for the investigations. The used data, of the urban network and underground cables, are proposed based on the data from [6]–[10]. Some of the network and cable data are given in appendix. The mathematical model of the network has been implemented

using the alternative transient program ATP/EMTP which is a popular simulation software package mainly intended for transient analysis applications [11]. The ATPDraw, a graphical pre-processor to ATP, has been used to construct the network elements using suitable graphical blocks/symbols, to plot the required figures and to write the required output data files in a suitable form to transfer it to Matlab [12] for the required analysis.

The investigations will be based on different simulation test cases of the medium voltage network including un-earthed neutral, compensated neutral, and compensated neutral with parallel neutral resistance networks. The performance of the techniques can be investigated easily by the comparison of the different test cases. The investigations will focus on the behavior of the fault currents through the sections of the faulted feeder.

The considered fault type is a SLGF (single line to ground fault in phase-a), initially with a fault resistance of 30Ω , occurred in the first underground-cable feeder, in section 3. The fault should be detected by indicators in the faulty sections; 1, 2 and 3 and on the same time should not be detected by the indicators in the healthy sections; 4, 5, 6, and 7.

Method 1 is mainly proposed for un-earthed neutral networks. The instantaneous residual currents for all sections (S1–S7), in the faulted feeder (CF1), are shown in Fig. 6, which presents their behavior during the first few milliseconds after the fault incidence (at 47 ms). The proposed fault indicators are presented in Fig. 7, in per unit with respect the highest fault current, in indicator (S3). Method 1 seems to be very selective with regard to earth fault indication. The residual current measured behind the fault, and also in healthy lateral branches of the faulty feeder, is very small compared to the points where fault current is expected to flow. Further, the fault indication along the path of the fault current seems to be fairly close to unity at all measurement locations. The simulation was made for the case when the instantaneous phase voltage is close to the maximum, hence producing the maximum expected transient amplitudes. In real cases, the fault may enter at lower instantaneous voltages. However, it is very likely that the start of the fault is initiated at a moment when there is a substantial voltage stress over the insulation.

Another issue that has to be taken into account with Method 1 is the required sampling frequency and associated signal processing. The sampling frequency in our simulated case was 10 kHz, which seems to be adequate for the applications in city networks, where thanks to the high capacitance of the cables, the transient frequencies are relatively low. The fault indication result can substantially be improved by using appropriate band-pass filtering techniques and appropriate averaging of the measured samples.

Method 2 is intended for compensated neutral networks, with neutral resistance connected in parallel to the compensation coil. The phasor residual currents for all sections (S1–S7), in the faulted feeder (CF1), are shown in Fig. 8, which presents their behavior before the fault incidence (at 0.407 s), after the fault incidence but before connecting the neutral resistance, and after connecting the resistance (at 1.007 s). The proposed fault indicators, in (4), are presented in Fig. 9, in per unit with respect the highest current change, found in indicator (S3). Also this method gives a clear difference between the faulty and non-faulty sections. The current change in non-faulty sections is almost

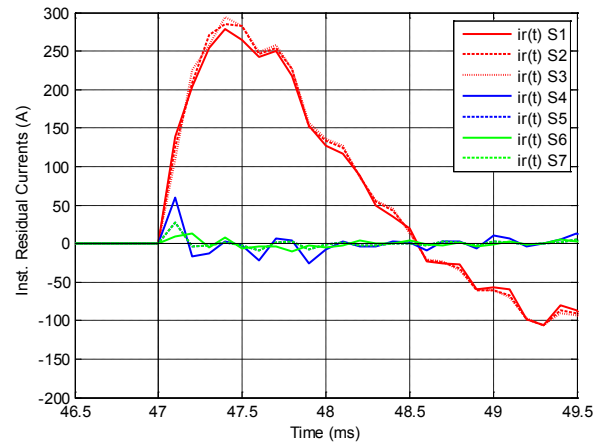


Fig. 6. The instantaneous residual currents for all sections (S1–S7) in the faulted feeder (CF1), in un-earthed network.

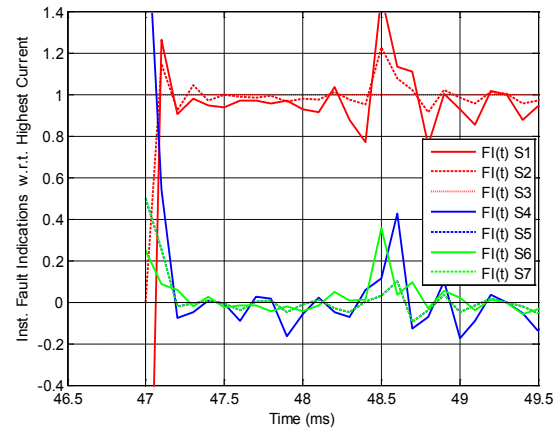


Fig. 7. The proposed fault indicators, in Method 1, in per unit with respect the highest fault indicator (S3), in un-earthed network.

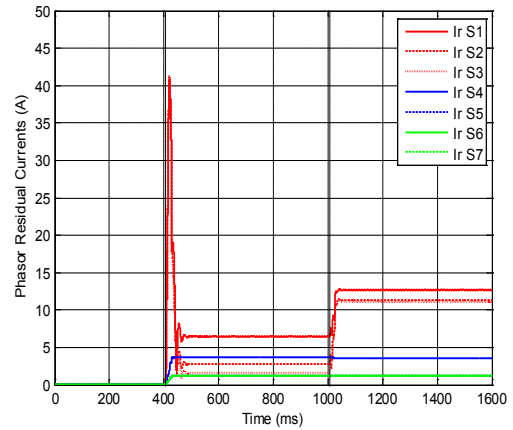


Fig. 8. The phasor residual currents for all sections (S1–S7), in the faulted feeder (CF1), in compensated un-earthed neutral, with neutral resistance connected in parallel with the compensation coil, network.

negligible. However, there seems to be a relatively high variation in the level of fault indication in the faulty sections. This is primarily due to large differences in the fault currents prior to the resistance switching. Hence, the setting of the indicator margin is more challenging in this case compared to Method 1. The method may be improved by measuring, instead of the total phasor change, only the resistive component change of the residual current. This requires, however, some reference of the direction of the resistive current. In conventional case, this reference is taken from the neutral voltage, which actually leads to the

commonly used directional relay principle. The phase reference taken from voltage measurement at the secondary substations could be replaced by using accurate time synchronization based on e.g. GPS. However, usually in city areas, many of the substations are underground or in the cellars, where the GPS signal is weak.

Method 3, also, is demonstrated here for compensated neutral, with neutral resistance connected in parallel with the compensation coil, networks. The phasor zero-sequence current changes, in (5), for all sections (S1–S7), in the faulted feeder (CF1), are shown in Fig. 10 and the corresponding phasor negative-sequence current changes, in (6), are shown in Fig. 11. The negative-sequence to zero-sequence current changes ratios are presented in Fig. 12, and the corresponding measured margin m , in (6), for all sections are presented in Fig. 13. The Method 3 seems to be more selective and robust than the Method 2. Negative sequence current changes seem to be negligible in the non-faulty sections. Also, they are similar in all the measurement locations along the fault current path. So it seems that this method has a good potential for further development. It is suggested here that the fault indicator should be based on the comparison of negative sequence current changes only, with the threshold of zero sequence current changes used for blocking against nuisance tripping of the fault indicator. Hence, according to the simulation results, the fault indicator algorithm could be simplified as follows:

$$\Delta I_0 > \Delta I_{0,set} \quad (7a)$$

$$\Delta I_n > \Delta I_{n,set} \quad (7b)$$

where the fault indication is set “TRUE” if both conditions are satisfied. The limit values should be taken so, that the setting for negative sequence current is well below the smallest fault current that is targeted to be detected. Since the change in zero sequence current only is used for general detection of the earth fault existence, its setting can be made somewhat more sensitive.

It should be noticed here, that although Method 3 is illustrated here for the case of resistor switching in compensated neutral network, it is equally applicable in the case on unearthed neutral. In this latter case, the comparison is made between the currents before and after the fault initiation.

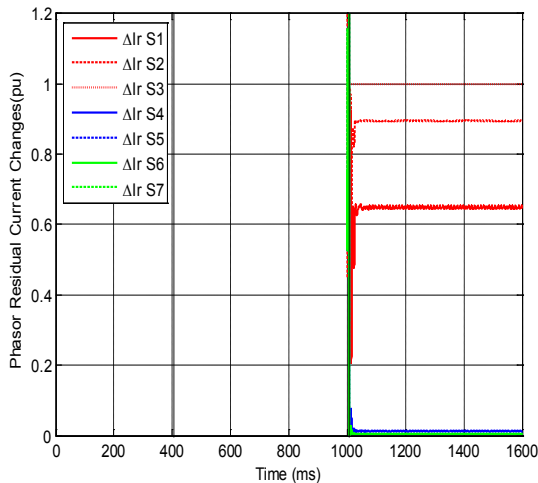


Fig. 9. The proposed fault indicators, in Method 2, in per unit with respect the highest fault indicator (S3), in compensated unearthed neutral, with neutral resistance connected in parallel with the compensation coil, network.

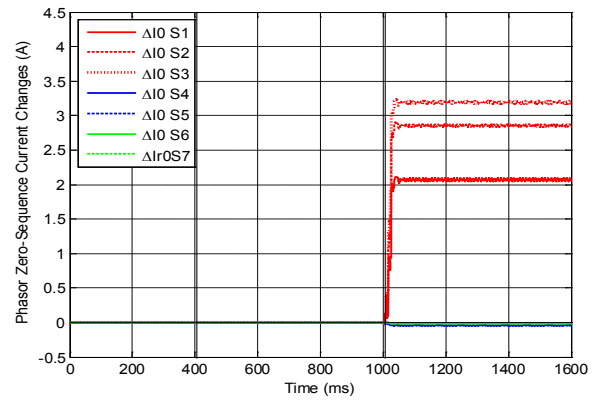


Fig. 10. The phasor zero-sequence current changes for all sections (S1–S7), in the faulted feeder (CF1), in compensated unearthed neutral, with neutral resistance connected in parallel with the compensation coil, network.

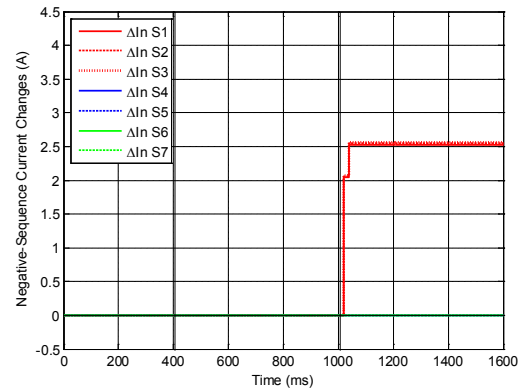


Fig. 11. The phasor negative-sequence current changes for all sections (S1–S7), in the faulted feeder (CF1), in compensated unearthed neutral, with neutral resistance connected in parallel with the compensation coil, network.

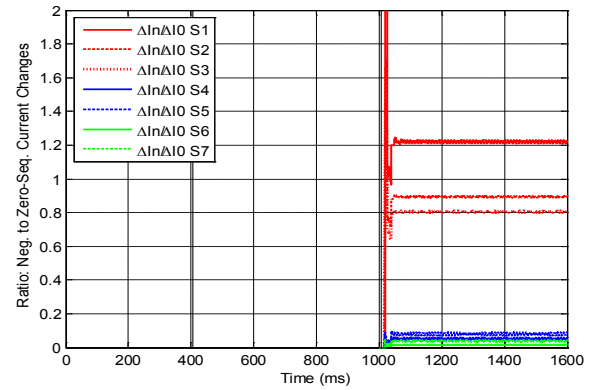


Fig. 12. The negative-sequence to zero-sequence current changes ratios.

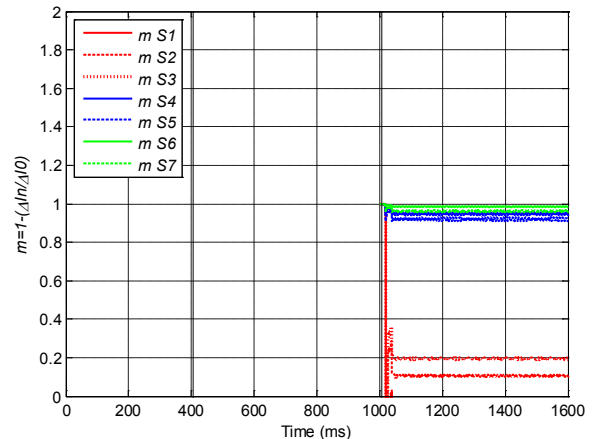


Fig. 13. The corresponding margin m , in (6), for all sections.

V. SUMMARY

The goal of the paper was to present simple fault indication techniques, which could easily be retrofitted at the various types and conditions of existing secondary substations in city or urban medium voltage distribution network conditions. The main limitation set to the methods was that they should be based on current measurements solely. This excludes the directional principles.

According to the simulation results, the Methods 1 and 3 seem to be the most promising. Their mutual superiority depends on the availability of measurement technology. Method 1 requires relatively high sampling frequency (10 kHz) and a large dynamic scale. On the other hand, the earth fault indication can be based on sum current measurement only. Method 1 also requires comparison of the measured quantities at the network control system level, and some digital filtering techniques employed at the DMS system, while processing the fault indicator measurements. These lead to the requirement that the measured data samples be transmitted from the secondary substation to the network control center.

Method 3 is simpler in the sense that it only utilizes local measurements and can provide a simple one digit indication of the fault existence. This method requires three phase current measurements to be combined, which may increase the measurement errors. However, the data sampling frequency can be low, since only the fundamental frequency signals are of interest. Also, the same current measurements can be used for both short circuit and earth fault indication, as long as the dynamic scale is large enough for sufficient resolution. If the quality of the Method 3 is required to be improved, the measured current changes can be communicated to the control center level for the comparison of their amplitudes.

VI. CONCLUSIONS

Reliable fault indication is the basic requirement for any fault management system in distribution networks. When developing the self-healing properties of the existing power systems, one of the biggest challenges is to adapt to the long life cycle of the secondary substations and to develop solutions that can be retrofitted to the various types and conditions of existing substations. To get the full benefits of distribution automation, the fault management should have full coverage. Hence, there is an urgent need for an affordable, but still reliable fault indication solution, which could be installed at the locations where full automation is not economically feasible. It is hoped that the methods presented in this paper can meet this challenge.

APPENDIX

The urban MV underground cable network data:

- Voltage: 20 kV
- Total length: 44 km
- Substation transformer: 50 MVA, 110/20 kV
- Number of feeders: 11
- Peak feeder load: 4 MVA
- Number of sections per feeder: 8
- Average section length: 0.5 km
- Number of load points per feeder: 8
- Load point LV transformer: 500 kVA, 20/0.4 kV
- Fault in section 3, in Feeder 1

Underground cable data:

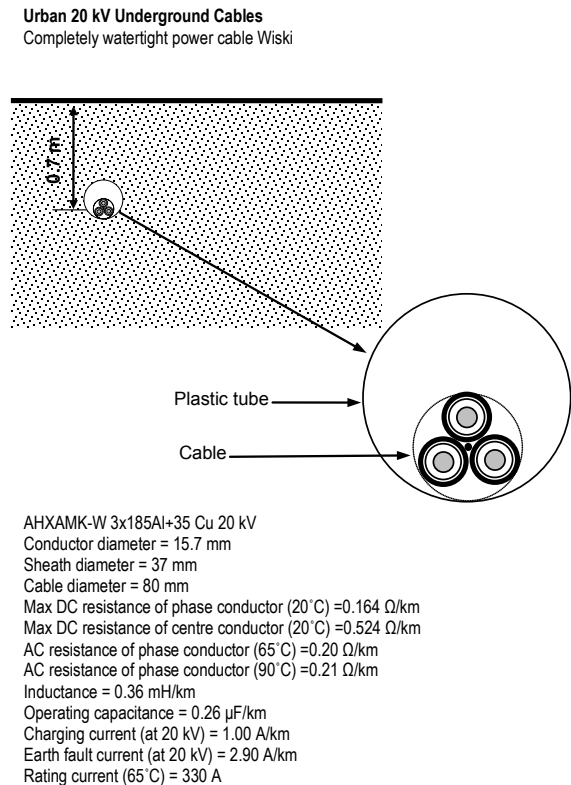


Fig. 14. The typical 20 kV urban underground cable data.

REFERENCES

- [1] A. Silvast, P. Heine, M. Lehtonen, K. Kivikko, A. Mäkinen, P. Järventausta, 2005, "Sähköjakelun keskeytyksestä aiheutuva haitta" (Outage costs in electrical distribution networks), In Finnish. Helsinki University of Technology, Tampere University of Technology.
- [2] B. E. Baarsma, J. P. Hop. "Pricing power outages in the Netherlands", *Energy* 34 (2009) 1378–1386
- [3] K. H. LaCommare and J. H. Eto, "Understanding the Cost of Power Interruptions to U.S. Electricity Consumers", Lawrence Berkeley National Laboratory, September 2004.
- [4] J. Jääskeläinen, "Customer Interruption Costs in the City Area", Master's thesis, Aalto university School of science and Technology, 2010.
- [5] O. Siirto, S. Hakala, M. Hyvärinen, P. Heine, M. Lehtonen, "Optimization of Distribution Automation in Urban Networks, " *International Review of Electrical Engineering (I.R.E.E)*, Vol. 8, N. 4, pp. 1324-1332, July-August 2013..
- [6] E. Lakervi and E. J. Holmes, *Electricity Distribution Network Design*, Second Edition, Peter Peregrinus Ltd. - on behalf of - the Institute of Electrical Engineers, London, U.K., 1995.
- [7] J. Elovaara and Y. Laiho, *Sähkölaitostekniikan Perusteet, Tekijät ja Otatieto Oy, Karisto Oy, Hämeenlinna, Finland, 1993.*
- [8] Prysmian Cables & Systems Finland. Information on: <http://www.prysmian.fi/index.html>
- [9] E. Lakervi and J. Partanen, *Sähköjakelutekniikka*, Gaudeamus Helsinki University Press / Otatieto, Helsinki, Finland, 2008.
- [10] M. Hyvärinen, "Electrical networks and economics of load density," Ph.D. dissertation, Dept. of Electrical Eng., Helsinki Univ. of Technology, TKK 146, Espoo, Finland, 2008.
- [11] Information at: <http://www.emtp.org/>
- [12] Information at: <http://www.mathworks.com/>
- [13] A. Nieminen, "Development of the automation at secondary substations", Master's thesis, Aalto University, 2010. (In Finnish).

BIOGRAPHIES



Matti Lehtonen (1959) was with VTT Energy, Espoo, Finland from 1987 to 2003, and since 1999 has been a professor at the Helsinki University of Technology (TKK), where he is now head of Power Systems and High Voltage Engineering.

Matti Lehtonen received both his Master's and Licentiate degrees in Electrical Engineering from Helsinki University of Technology in 1984 and 1989, respectively, and the Doctor of Technology degree from Tampere University of Technology in 1992.

His main activities include power system planning and asset management, power system protection including earth fault problems, harmonic related issues and applications of information technology in distribution systems.



Osmo Siirto (1962) received the M.S. degree in Electrical Engineering from Helsinki University Aalto University (formerly Helsinki University of Technology), Espoo, Finland, in 1990. Since 2009 he has also been a D.Sc. student in Aalto University at Department of Electrical Engineering. From 1990, he has been working in many fields of electrical engineering in Helsinki Energy and Helen Electricity Network Ltd. (DSO subsidiary of Helsinki Energy), Helsinki, including network planning, network operation, distribution automation and asset management. At present, he is working as Unit Manager of Distribution network

at Helen Electricity Network Ltd. He is also Task Manager of Task "Self Healing City Networks" in Finnish Smart Grid and Energy Market Program SGEM. His research interests include asset management, distribution network planning and operation, automation systems and smart grids.



Mohamed F. Abdel-Fattah was born in Qualiobia, Egypt on June 11, 1972. He received his B.Sc. in 1995 with distinction and first class honors from Zagazig University, Egypt and was appointed as a teaching assistant and researcher with the Faculty of Engineering. From the same university, he received his M.Sc. degree in 2000 and Ph.D. degree in 2006 and was appointed as a lecturer with the Department of Electrical Power and Machines Engineering.

Recently, he joined Aalto University, Finland, as a post-doctoral researcher with the power systems group in the Department of Electrical

Engineering. His main research activities are related to power system protection, including earth-fault detection, diagnosis and location using transient and fast transient-based algorithms. His current research topic is the development of intelligent protection systems for the self-healing capability of smart grids.